

Short-flow-time expansion of non-singlet twist-two operators at next-to-next-to-leading order QCD

Robert V. Harlander¹, Jonas T. Kohnen¹, and Andrea Shindler^{1,2,3}

¹*TTK, RWTH Aachen University, 52056 Aachen, Germany*

²*Nuclear Science Division, Lawrence Berkeley National Laboratory, Berkeley, CA 94720
USA*

³*Department of Physics, University of California, Berkeley, CA 94720, USA*

Abstract

The gradient-flow formalism provides a framework for the direct determination of moments of parton distribution functions (PDFs) from lattice QCD calculations. Their conversion from the gradient-flow scheme to $\overline{\text{MS}}$ requires the matching coefficients of the short-flow-time expansion, which can be computed perturbatively. We determine these coefficients for the first six non-singlet PDF moments up to next-to-next-to-leading order in the strong coupling.

Contents

1	Introduction	1
2	Theoretical framework	3
2.1	Twist-two non-singlet operators	3
2.2	The QCD gradient flow	4
2.3	Calculation of the matching coefficients	5
3	Results	8
4	Conclusions	11
A	Definition of the gradient flow	11
B	Renormalization constants	12
C	Ancillary file	14

1 Introduction

Theoretical cross-section predictions for hadronic scattering processes rely on the factorization [1] into a perturbatively accessible partonic subprocess and non-perturbative contributions associated with the initial- and final-state hadrons. Those related to the initial

state are encoded in the parton distribution functions (PDFs), which describe the probability of finding a parton carrying a fraction x of the hadron momentum. Their dependence on the factorization scale Q is governed by the Dokshitzer-Gribov-Lipatov-Altarelli-Parisi (DGLAP) evolution equations [2–4], whose kernels are the splitting functions.

A quantitative determination of the PDFs requires both the perturbative splitting functions and suitable non-perturbative initial conditions, i.e. the x dependence of the parton densities at a reference scale Q_0 . The splitting functions are calculable in perturbation theory and are known up to three-loop order [5, 6], with partial four-loop results now available [7–13]. The initial conditions, on the other hand, are typically obtained by fitting phenomenological parametrizations of PDFs to data, although significant progress has recently been made toward their direct computation using lattice QCD.

A first-principles determination of PDFs is indeed highly desirable. It would clarify the non-perturbative structure of QCD, provide systematically improvable input for collider phenomenology, and supply theoretical benchmarks that are independent of global fits and could be combined with them to increase precision. Such progress would strengthen precision tests of the Standard Model (SM) and improve the sensitivity to possible signals of physics beyond-the-Standard Model (BSM) at present and future facilities [14–16].

Lattice QCD offers a natural framework for such a determination. While lattice calculations have achieved remarkable precision in many areas of hadronic physics, obtaining phenomenologically relevant results for PDFs remains challenging. The main reason for this is that PDFs are defined through light-cone correlations, whereas lattice gauge theory is formulated in Euclidean space. Several theoretical frameworks, such as quasi-PDFs, pseudo-PDFs, and related approaches provide access to the x -dependence of PDFs from Euclidean correlators [17–26]. These methods establish a systematic connection between Euclidean observables and light-cone parton physics, although they require careful control of short-distance effects and hadron momenta to ensure reliable access to the light-cone regime.

An alternative and long-established approach focuses on the Mellin moments $\langle x^{n-1} \rangle$ ($n \in \mathbb{N}$) of the PDFs, which can be expressed as matrix elements of local twist-two operators accessible on the lattice. However, the reduced symmetry of discretized space-time compared to the continuum leads to mixing of these operators with lower-dimensional ones, resulting in divergences that scale as inverse powers of the lattice spacing a [27]. This limits the attainable precision for higher moments, and conventional lattice determinations beyond the lowest few [28–32] remain impractical.

Recently, it was shown [33] that these power divergences can be avoided entirely by employing the gradient-flow formalism (GFF) [34–37]. In this approach, high-momentum modes of the flowed fields are exponentially suppressed by the flow time t , rendering matrix elements of composite operators ultra-violet (UV)-finite and admitting a well-defined continuum limit. Since the GFF preserves the full rotational symmetry of Euclidean space, operators can be organized into irreducible representations of $O(4)$. Mixing with lower-dimensional operators is absent for $t > 0$, and so are the associated power divergences. Building on this property, Ref. [33] proposed a new approach that employs flowed twist-two operators to determine higher Mellin moments of the PDFs.

To relate the flowed matrix elements at finite flow time $t > 0$ to the standard renormalization scheme used in phenomenology, one must convert them to the $\overline{\text{MS}}$ scheme defined at $t = 0$. This is achieved through a short-flow-time expansion (SFTX) [36, 38, 39], in which the flowed twist-two operators are expressed as a series of local operators renormalized in the $\overline{\text{MS}}$ scheme and multiplied by perturbatively calculable matching coefficients. At next-to-leading order (NLO) in QCD, the matching coefficients for the moments $\langle x^{n-1} \rangle$ have been computed for general $n \in \mathbb{N}$ [33, 40]. From other applications of the SFTX, it is known that higher-order corrections to the matching coefficients are important in several respects [41–43]. First and foremost, as in any perturbative calculation, they are crucial for reducing the systematic uncertainties from missing higher orders, of course. But in the context of the SFTX, they are also found to stabilize the extrapolation to $t \rightarrow 0$.

For this reason, in the present work we extend the calculation of the matching coefficients for the PDFs to next-to-next-to-leading order (NNLO) in QCD, focusing on non-singlet flowed twist-two operators up to $n = 6$. The resulting coefficients have already been employed in the first numerical determinations of the moments of the valence pion PDF on ensembles generated by the OpenLat initiative [44–47]. Preliminary results were presented in Ref. [48], and the complete analyses are reported in Refs. [49, 50], which use the results of the present NNLO calculation to perform the matching to the $\overline{\text{MS}}$ scheme.

The remainder of this paper is structured as follows. The theoretical framework is outlined in Section 2, the main results are presented in Section 3, and conclusions are given in Section 4. The appendix collects the essentials of the GFF, as well as a description of the contents of the ancillary files associated with this paper.

2 Theoretical framework

2.1 Twist-two non-singlet operators

The quantities of interest in this work are the twist-two quark bilinear operators¹

$$\widehat{O}_{\{\mu_1 \dots \mu_n\}}^{rs}(x) = \bar{\psi}^r(x) \gamma_{\{\mu_1} \overleftrightarrow{D}_{\mu_2}(x) \dots \overleftrightarrow{D}_{\mu_n\}}(x) \psi^s(x) - \text{traces}, \quad (2.1)$$

built from quarks of flavors r and s . Here, $\overleftrightarrow{D}_\mu = (D_\mu - \overleftarrow{D}_\mu)/2$ is the symmetrized covariant derivative, with the right- and left-acting derivatives D_μ and \overleftarrow{D}_μ . The braces indicate normalized symmetrization over Lorentz indices, and the trace subtraction enforces $\delta_{\alpha\beta} \widehat{O}_{\mu_1 \dots \mu_n} = 0$ for any distinct $\alpha, \beta \in \{\mu_1, \dots, \mu_n\}$. In the continuum, these operators transform irreducibly under the Euclidean rotation group $O(4)$ and therefore renormalize multiplicatively. In the calculation of the matching coefficients we work with massless quarks and off-diagonal operators \widehat{O}^{rs} with $r \neq s$, which correspond to inserting a particular traceless $SU(n_f)$ generator, where n_f is the number of quark flavors. Since all non-singlet flavor structures, including phenomenologically relevant combinations such as $\widehat{O}^{uu} - \widehat{O}^{dd}$ or $\widehat{O}^{uu} + \widehat{O}^{dd} - 2\widehat{O}^{ss}$, are obtained by choosing other traceless generators and have

¹We adopt the same notation for these operators as in Refs. [49, 50] for consistency.

the same renormalization pattern, the resulting matching coefficients apply universally to every non-singlet operator.

For later use we also introduce their Fourier transform,

$$\widehat{O}(q) = \int d^4y e^{iqy} \widehat{O}(y), \quad (2.2)$$

with $\widehat{O} \equiv \widehat{O}(q=0)$ for the corresponding local operator.

For a hadron $h(p)$ with four-momentum p , the renormalized matrix elements of these operators determine the Mellin moments of the PDFs

$$Z_n \langle h(p) | \widehat{O}_{\{\mu_1 \dots \mu_n\}}^{qq} | h(p) \rangle (\mu) = 2(p_{\mu_1} \dots p_{\mu_n} - \text{traces}) \langle x^{n-1} \rangle_q^h(\mu), \quad (2.3)$$

where the renormalization constants Z_n are collected in Section B up to $n = 6$ in the $\overline{\text{MS}}$ scheme, and μ is the renormalization scale. The $(n-1)^{\text{th}}$ Mellin moment is defined as

$$\langle x^{n-1} \rangle_q^h(\mu) = \int_0^1 dx x^{n-1} [q^h(x, \mu) + (-1)^n \bar{q}^h(x, \mu)], \quad (2.4)$$

where $q^h(x, \mu)$ and $\bar{q}^h(x, \mu)$ are the quark and antiquark distributions in the hadron h at factorization scale μ , respectively. This establishes a direct connection between PDF moments and matrix elements of local renormalized operators. A lattice calculation of $\langle h(p) | \widehat{O}_{\{\mu_1 \dots \mu_n\}}^{qq} | h(p) \rangle$ therefore provides non-perturbative access to $\langle x^{n-1} \rangle_q^h$.

Progress in this direction has long been limited by the loss of full rotational symmetry once a lattice regulator is introduced. It causes the traceless operators in Eq. (2.1) to mix with operators of lower dimension [27–29], giving rise to power divergences in the lattice spacing. For $n \leq 4$ this problem can be partially mitigated by forming specific linear combinations of the operators $\widehat{O}_{\{\mu_1 \dots \mu_n\}}^{rs}$ that transform according to irreducible representations of the hypercubic group $\text{H}(4)$. However, this procedure requires the use of boosted hadrons to project the correct tensor structures, which leads to a severe degradation of the signal-to-noise ratio in the relevant correlation functions. As a consequence, calculations of $\langle x^{n-1} \rangle$ for $n > 4$ have been effectively out of reach, and even the moments for $n = 3$ and $n = 4$ have traditionally suffered from very large statistical uncertainties.

To solve this problem a strategy has been proposed in Ref. [33], based on the GFF [34–37], which makes it possible to take the continuum limit while restoring rotational symmetry. This crucially eliminates the power-divergent mixings that affect the standard lattice operators. Once the flowed matrix elements are obtained, the matching to the physical (unflowed) matrix elements can be performed entirely in the continuum using the SFTX [36, 38, 39]. In this work we provide the required matching coefficients at NNLO for the non-singlet flavor sector, covering moments up to $n = 6$.

2.2 The QCD gradient flow

In the GFF the gauge and fermion fields of QCD are extended into an auxiliary fifth coordinate, the flow time t [35–37]. Their evolution in t is governed by Lorentz-covariant

first-order differential equations, with the boundary condition that at $t = 0$ the flowed fields coincide with the ordinary four-dimensional QCD fields. Further details on the flow equations are given in Section A.

A key property of the GFF is that composite operators built from flowed fields at $t > 0$ are finite once the standard QCD parameters and the flowed fermion fields are renormalized [36, 37, 51]. In our case this requires only the renormalization of the strong coupling (in the $\overline{\text{MS}}$ scheme) and of the flowed quark fields $\chi^q(t)$. For the latter we use the ringed scheme [52], defined by²

$$\mathring{Z}_\chi \sum_{q=1}^{n_f} \langle \overline{\chi}^q(t) \overleftrightarrow{\mathcal{D}}(t) \chi^q(t) \rangle = -\frac{n_c n_f}{(4\pi t)^2}, \quad (2.5)$$

where $\overleftrightarrow{\mathcal{D}}_\mu = (\mathcal{D}_\mu - \overleftarrow{\mathcal{D}}_\mu)/2$ is the symmetrized flowed covariant derivative in the fundamental representation (see Eq. (A.7)). The explicit expression for \mathring{Z}_χ is given in Eqs. (B.5) to (B.7).

With these ingredients one defines the flowed twist-two operators

$$\widehat{\mathcal{O}}_{\{\mu_1 \dots \mu_n\}}^{rs}(t, x) = \mathring{Z}_\chi \overline{\chi}^r(t, x) \gamma_{\{\mu_1} \overleftrightarrow{\mathcal{D}}_{\mu_2}(t, x) \dots \overleftrightarrow{\mathcal{D}}_{\mu_n\}}(t, x) \chi^s(t, x). \quad (2.6)$$

For sufficiently short flow time, these operators satisfy a SFTX relating them to the ordinary twist-two operators of Eq. (2.1):

$$\widehat{\mathcal{O}}_{\{\mu_1 \dots \mu_n\}}^{rs}(t, x) = \zeta_n^{\text{B}}(t) \widehat{\mathcal{O}}_{\{\mu_1 \dots \mu_n\}}(x), \quad (2.7)$$

which holds up to terms that vanish in the limit $t \rightarrow 0$. For the non-singlet case considered here the matching is multiplicative: each $(n-1)^{\text{th}}$ moment requires a single coefficient ζ_n .

The superscript ‘‘B’’ indicates that these matching coefficients contain ultraviolet divergences associated with the regular operators in Eq. (2.1). Renormalizing those operators yields the finite coefficients

$$\zeta_n(t, \mu) = (Z_n \zeta_n^{\text{B}}(t))(\mu), \quad (2.8)$$

where μ is the renormalization scale and Z_n are the renormalization constants of Eq. (2.3) (see Section B).

2.3 Calculation of the matching coefficients

For the determination of the matching coefficients ζ_n , we apply the method of projectors [54–56]. Defining

$$P_{\mu_1 \dots \mu_n}[O] = N_n (\partial_p - \partial_k)_{\mu_2 \dots \mu_n}^{n-1} \text{Tr} [\gamma_{\mu_1} \langle \psi_q(p) | O(p+k) | \psi_{q'}(k) \rangle] \Big|_{\substack{k=p=0 \\ m_q=m_{q'}=0}}, \quad (2.9)$$

where the derivatives ∂_p, ∂_k w.r.t. the quark momenta and the subsequent nullification of these momenta and the quark masses $m_q, m_{q'}$ are taken *before* any loop integration. With suitably chosen normalization factors N_n , it follows that

$$P_{\mu_1 \dots \mu_n}[\widehat{\mathcal{O}}_{\{\mu_1 \dots \mu_n\}}] = \delta_{nm} \quad (2.10)$$

²Note the factor of two between the definition of $\overleftrightarrow{\mathcal{D}}_\mu$ used here and in Ref. [53].

at tree-level, which can easily be verified using the Feynman rules of the operators in Eq. (2.1).³ Up to $n = 6$, it is

$$\begin{aligned}
N_1 &= -\frac{1}{4D}, \\
N_2 &= -\frac{i}{2(D+2)(D-1)}, \\
N_3 &= -\frac{3}{4(D+4)D(D-1)}, \\
N_4 &= -\frac{i}{(D+6)(D+1)D(D-1)}, \\
N_5 &= -\frac{5}{4(D+8)(D+2)(D+1)D(D-1)}, \\
N_6 &= -\frac{3i}{2(D+10)(D+3)(D+2)(D+1)D(D-1)},
\end{aligned} \tag{2.11}$$

where

$$D = 4 - 2\epsilon \tag{2.12}$$

is the space-time dimension used for regularizing the momentum integrals [57]. At higher orders, all occurring loop integrals on the l.h.s. of Eq. (2.10) are scaleless and thus vanish in dimensional regularization, which means that this relation actually holds to all orders in perturbation theory.

Applying the projectors of Eq. (2.10) onto Eq. (2.7) therefore gives the bare matching coefficients [53, 56]

$$\zeta_n^{\text{B}}(t) = P_{\mu_1 \dots \mu_n} [\widehat{\mathcal{O}}_{\{\mu_1 \dots \mu_n\}}(t)]. \tag{2.13}$$

It is important to note that we only included physical operators on the r.h.s. of Eq. (2.7), as they are the only ones that contribute to physical matrix elements of that relation. For off-shell matrix elements as required for the method of projectors, unphysical operators have to be taken into account, in particular those involving total derivatives. The choice of the projectors in Eq. (2.9) is such that they implicitly eliminate total-derivative operators.

The calculation of the matching coefficients according to Eq. (2.13) is based on an updated version of the setup described in Ref. [53]. The Feynman diagrams are generated using *qgraf* [58, 59]. A generic diagram that contributes to the r.h.s. of Eq. (2.13) is shown in Fig. 1; the number of gluons attached to the operator $\widehat{\mathcal{O}}_{\{\mu_1 \dots \mu_n\}}$ is $\leq n - 1$. Specific examples for diagrams contributing up to NNLO are shown in Fig. 2 (a)–(f). The number of contributing diagrams is shown in Table 1.

Using *tapir/exp* [60–63], we insert the Feynman rules and identify the topologies of the associated Feynman integrals. The resulting expression is evaluated algebraically with the help of *FORM* [64, 65] until it contains only scalar integrals, multiplied by rational functions depending on the space-time parameter D , see Eq. (2.12). The scalar integrals are reduced using integration-by-parts relations [66] with the help of *Kira* [67, 68] and *FireFly* [69, 70]. At NNLO, this results in only six (NLO: one) master integrals which are known analytically [56].

³In practice, we generate the Feynman rules as well as the corresponding projectors automatically using in-house software.

Table 1: Number of diagrams contributing to the r.h.s. of Eq. (2.13) through NNLO for specific values of n .

order	$n = 1$	$n = 2$	$n = 3$	$n = 4$	$n \geq 5$
LO	1	1	1	1	1
NLO	10	14	15	15	15
NNLO	375	737	798	804	805

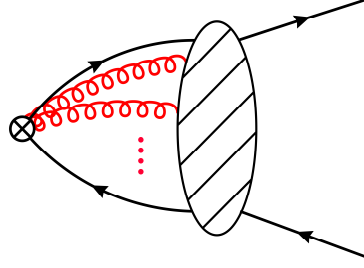


Figure 1: Generic form of the diagrams contributing to the r.h.s. of Eq. (2.13). All Feynman diagrams in this paper were created using *FeynGame* [71, 72].

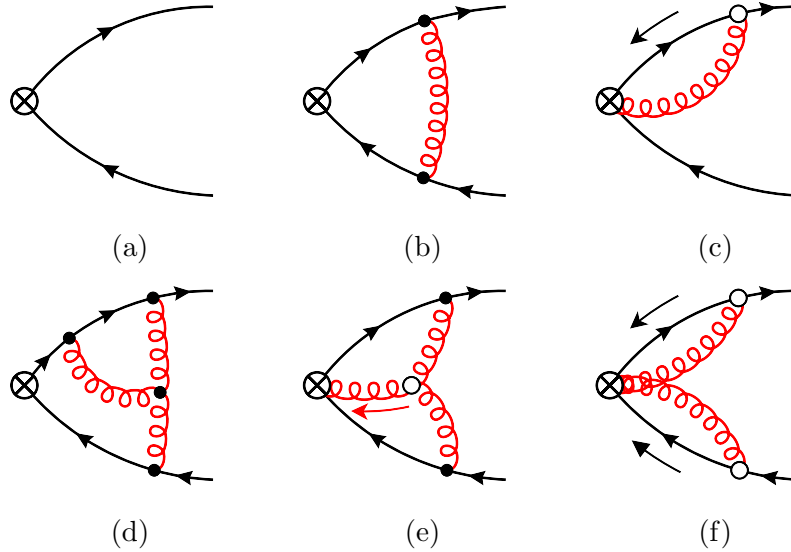


Figure 2: Examples for diagrams contributing to the r.h.s. of Eq. (2.13). (a): tree-level diagram contributing for all $n \geq 1$; (b) and (c): diagrams contributing at NLO for all $n \geq 1$ and $n \geq 2$, respectively; (d), (e), (f): diagrams contributing at NNLO for all $n \geq 1, 2, 3$, respectively. Straight lines denote quarks, curly lines gluons; flow lines are marked by an arrow next to them, which denotes the flow direction; filled/hollow vertex symbols denote regular/flowed vertices; the symbol \otimes denotes one of the operators of Eq. (2.6).

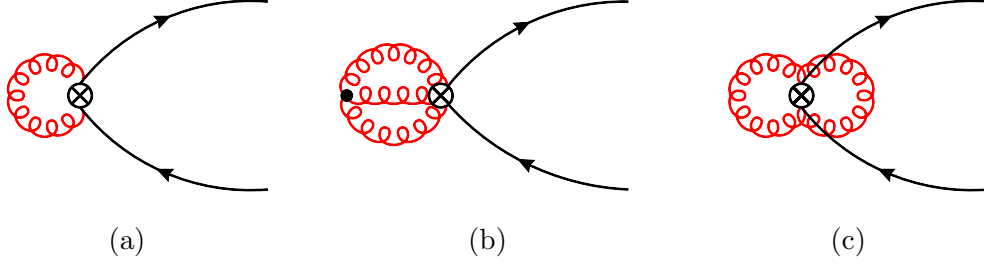


Figure 3: Examples for diagrams contributing to the r.h.s. of Eq. (2.13). (a): diagram contributing at NLO for all $n \geq 3$; (b), (c): diagram contributing at NNLO for all $n \geq 4, 5$, respectively. The notation is the same as in Fig. 2. Note that due to the flow time associated with the operator vertex, these diagrams do not involve scaleless integrals and are therefore non-zero.

3 Results

We provide the results for a general gauge group, with the Casimirs of the fundamental and adjoint representation denoted by C_F and C_A , respectively, the trace normalization of the fundamental generators denoted by T_R , and n_f the number of quark flavors. In QCD, it is

$$C_F = \frac{4}{3}, \quad C_A = 3, \quad T_R = \frac{1}{2}. \quad (3.1)$$

Furthermore, we define

$$a_s(\mu) = \frac{g^2(\mu)}{4\pi^2}, \quad (3.2)$$

where $g(\mu)$ is the strong coupling in the $\overline{\text{MS}}$ scheme, evaluated at the renormalization scale μ , see Eq. (B.1), and

$$L_{\mu t} = \ln 2\mu^2 t + \gamma_E, \quad (3.3)$$

where $\gamma_E = 0.577215\dots$ is the Euler-Mascheroni constant. Adopting the ringed scheme for the flowed quark fields, we find the following matching coefficients:

$$\begin{aligned} \zeta_1(t, \mu) = & 1 + a_s C_F \left(\frac{1}{8} - \ln 2 - \frac{3}{4} \ln 3 \right) \\ & + a_s^2 \left\{ \frac{1}{16} c_\chi^{(2)} + C_F^2 \left(-\frac{41}{128} - \frac{5}{32} \zeta(2) + \frac{3}{8} \ln 2 + \frac{1}{4} \ln^2 2 - \frac{3}{32} \ln 3 + \frac{3}{2} \text{Li}_2(1/4) \right) \right. \\ & + C_A C_F \left(-\frac{763}{384} - \frac{5}{32} \zeta(2) - \frac{13}{4} \ln 2 + \frac{1}{4} \ln^2 2 + \frac{27}{8} \ln 3 + \frac{21}{16} \text{Li}_2(1/4) \right) \\ & + C_F T_R n_f \left(\frac{35}{96} + \frac{1}{8} \zeta(2) \right) + L_{\mu t} \left[C_A C_F \left(-\frac{11}{12} \ln 2 - \frac{11}{16} \ln 3 + \frac{11}{96} \right) \right. \\ & \left. \left. + C_F T_R n_f \left(\frac{1}{3} \ln 2 + \frac{1}{4} \ln 3 - \frac{1}{24} \right) \right] \right\} + \mathcal{O}(a_s^3), \quad (3.4) \end{aligned}$$

$$\zeta_2(t, \mu) = 1 + a_s C_F \left(\frac{1}{72} - \ln 2 - \frac{3}{4} \ln 3 + \frac{2}{3} L_{\mu t} \right)$$

$$\begin{aligned}
& + a_s^2 \left\{ \frac{c_\chi^{(2)}}{16} + C_F^2 \left(\frac{2687}{10368} - \frac{13}{96} \zeta(2) + \frac{865}{216} \ln 2 - \frac{245}{96} \ln 3 + \frac{1}{4} \ln^2 2 + \frac{137}{144} \text{Li}_2(1/4) \right) \right. \\
& + C_A C_F \left(-\frac{12433}{10368} - \frac{49}{288} \zeta(2) - \frac{91}{54} \ln 2 + \frac{7}{6} \ln 3 + \frac{1}{4} \ln^2 2 + \frac{163}{144} \text{Li}_2(1/4) \right) \\
& + C_F n_f T_R \left(\frac{401}{2592} + \frac{1}{72} \zeta(2) \right) \\
& + L_{\mu t} \left[C_F^2 \left(-\frac{1}{4} - \frac{2}{3} \ln 2 - \frac{1}{2} \ln 3 \right) + C_A C_F \left(\frac{763}{864} - \frac{11}{12} \ln 2 - \frac{11}{16} \ln 3 \right) \right. \\
& \quad \left. + C_F n_f T_R \left(-\frac{65}{216} + \frac{1}{3} \ln 2 + \frac{1}{4} \ln 3 \right) \right] \\
& \left. + L_{\mu t}^2 \left[\frac{2}{9} C_F^2 + \frac{11}{36} C_A C_F - \frac{1}{9} C_F n_f T_R \right] \right\} + \mathcal{O}(a_s^3), \tag{3.5}
\end{aligned}$$

$$\begin{aligned}
\zeta_3(t, \mu) & = 1 + a_s C_F \left(-\frac{11}{288} - \ln 2 - \frac{3}{4} \ln 3 + \frac{25}{24} L_{\mu t} \right) \\
& + a_s^2 \left\{ \frac{c_\chi^{(2)}}{16} + C_F^2 \left(\frac{42023}{165888} - \frac{119}{1152} \zeta(2) + \frac{3145}{1152} \ln 2 - \frac{1393}{768} \ln 3 + \frac{1}{4} \ln^2 2 \right. \right. \\
& \quad \left. + \frac{119}{144} \text{Li}_2(1/4) \right) + C_A C_F \left(-\frac{1225}{2592} - \frac{227}{1152} \zeta(2) + \frac{527}{576} \ln 2 - \frac{979}{768} \ln 3 + \frac{1}{4} \ln^2 2 \right. \\
& \quad \left. + \frac{541}{576} \text{Li}_2(1/4) \right) + C_F n_f T_R \left(\frac{559}{20736} - \frac{7}{144} \zeta(2) \right) \\
& + L_{\mu t} \left[C_F^2 \left(-\frac{385}{1152} - \frac{25}{24} \ln 2 - \frac{25}{32} \ln 3 \right) + C_A C_F \left(\frac{4159}{3456} - \frac{11}{12} \ln 2 - \frac{11}{16} \ln 3 \right) \right. \\
& \quad \left. + C_F n_f T_R \left(-\frac{101}{216} + \frac{1}{3} \ln 2 + \frac{1}{4} \ln 3 \right) \right] \\
& \left. + L_{\mu t}^2 \left[\frac{625}{1152} C_F^2 + \frac{275}{576} C_A C_F - \frac{25}{144} C_F n_f T_R \right] \right\} + \mathcal{O}(a_s^3), \tag{3.6}
\end{aligned}$$

$$\begin{aligned}
\zeta_4(t, \mu) & = 1 + a_s C_F \left(-\frac{551}{7200} - \ln 2 - \frac{3}{4} \ln 3 + \frac{157}{120} L_{\mu t} \right) \\
& + a_s^2 \left\{ \frac{c_\chi^{(2)}}{16} + C_F^2 \left(\frac{145703293}{725760000} - \frac{2827}{28800} \zeta(2) + \frac{313751}{112000} \ln 2 - \frac{7028017}{4032000} \ln 3 + \frac{1}{4} \ln^2 2 \right. \right. \\
& \quad \left. + \frac{1997}{2880} \text{Li}_2(1/4) \right) + C_A C_F \left(-\frac{6179}{448000} - \frac{1489}{7200} \zeta(2) + \frac{905137}{336000} \ln 2 - \frac{1018799}{336000} \ln 3 \right. \\
& \quad \left. + \frac{1}{4} \ln^2 2 + \frac{10123}{9600} \text{Li}_2(1/4) \right) + C_F n_f T_R \left(-\frac{57059}{864000} - \frac{67}{720} \zeta(2) \right) \\
& + L_{\mu t} \left[C_F^2 \left(-\frac{37381}{86400} - \frac{157}{120} \ln 2 - \frac{157}{160} \ln 3 \right) + C_A C_F \left(\frac{8213}{5760} - \frac{11}{12} \ln 2 - \frac{11}{16} \ln 3 \right) \right. \\
& \quad \left. + C_F n_f T_R \left(-\frac{53}{90} + \frac{1}{3} \ln 2 + \frac{1}{4} \ln 3 \right) \right] \\
\end{aligned}$$

$$+ L_{\mu t}^2 \left[\frac{24649}{28800} C_F^2 + \frac{1727}{2880} C_A C_F - \frac{157}{720} C_F n_f T_R \right] \Big\} + \mathcal{O}(a_s^3), \quad (3.7)$$

$$\begin{aligned} \zeta_5(t, \mu) = & 1 + a_s C_F \left(-\frac{6163}{57600} - \ln 2 - \frac{3}{4} \ln 3 + \frac{91}{60} L_{\mu t} \right) \\ & + a_s^2 \left\{ \frac{c_\chi^{(2)}}{16} + C_F^2 \left(-\frac{208404649}{8709120000} - \frac{127}{1600} \zeta(2) + \frac{150325607}{72576000} \ln 2 - \frac{8869939}{8064000} \ln 3 \right. \right. \\ & + \frac{1}{4} \ln^2 2 + \frac{10441}{14400} \text{Li}_2(1/4) \Big) + C_A C_F \left(\frac{415266493}{870912000} - \frac{2129}{9600} \zeta(2) + \frac{160526033}{36288000} \ln 2 \right. \\ & - \frac{301797451}{64512000} \ln 3 + \frac{1}{4} \ln^2 2 + \frac{1563}{1600} \text{Li}_2(1/4) \Big) + C_F n_f T_R \left(-\frac{722059}{5184000} - \frac{23}{180} \zeta(2) \right) \\ & + L_{\mu t} \left[C_F^2 \left(-\frac{361949}{691200} - \frac{91}{60} \ln 2 - \frac{91}{80} \ln 3 \right) + C_A C_F \left(\frac{14717}{9216} - \frac{11}{12} \ln 2 - \frac{11}{16} \ln 3 \right) \right. \\ & \left. + C_F n_f T_R \left(-\frac{7891}{11520} + \frac{1}{3} \ln 2 + \frac{1}{4} \ln 3 \right) \right] \\ & \left. + L_{\mu t}^2 \left[\frac{8281}{7200} C_F^2 + \frac{1001}{1440} C_A C_F - \frac{91}{360} C_F n_f T_R \right] \right\} + \mathcal{O}(a_s^3), \quad (3.8) \end{aligned}$$

$$\begin{aligned} \zeta_6(t, \mu) = & 1 + a_s C_F \left(-\frac{372377}{2822400} - \ln 2 - \frac{3}{4} \ln 3 + \frac{709}{420} L_{\mu t} \right) \\ & + a_s^2 \left\{ \frac{c_\chi^{(2)}}{16} + C_F^2 \left(-\frac{1120571951063}{3651056640000} - \frac{5941}{78400} \zeta(2) + \frac{95875723}{50935500} \ln 2 - \frac{24927078637}{34771968000} \ln 3 \right. \right. \\ & + \frac{1}{4} \ln^2 2 + \frac{190727}{235200} \text{Li}_2(1/4) \Big) + C_A C_F \left(\frac{116671287151}{134120448000} - \frac{321851}{1411200} \zeta(2) \right. \\ & + \frac{177652851}{30184000} \ln 2 - \frac{424246536023}{69543936000} \ln 3 + \frac{1}{4} \ln^2 2 + \frac{123721}{117600} \text{Li}_2(1/4) \Big) \\ & + C_F n_f T_R \left(-\frac{355534709}{1778112000} - \frac{197}{1260} \zeta(2) \right) \\ & + L_{\mu t} \left[C_F^2 \left(-\frac{102996011}{169344000} - \frac{709}{420} \ln 2 - \frac{709}{560} \ln 3 \right) \right. \\ & + C_A C_F \left(\frac{8409979}{4838400} - \frac{11}{12} \ln 2 - \frac{11}{16} \ln 3 \right) + C_F n_f T_R \left(-\frac{925361}{1209600} + \frac{1}{3} \ln 2 + \frac{1}{4} \ln 3 \right) \Big] \\ & \left. + L_{\mu t}^2 \left[\frac{502681}{352800} C_F^2 + \frac{7799}{10080} C_A C_F - \frac{709}{2520} C_F n_f T_R \right] \right\} + \mathcal{O}(a_s^3), \quad (3.9) \end{aligned}$$

where $\text{Li}_2(z)$ is the dilogarithm, $\zeta(2) = \text{Li}_2(1) = \pi^2/6$, and $a_s = a_s(\mu)$. Through NLO, our results agree with those of Ref. [33], where expressions for general n were first presented. For $n = 1$, the operator in Eq. (2.1) reduces to the vector current, whose matching coefficient is known through NNLO from Ref. [73]. The case $n = 2$ corresponds to the quark kinetic operator, with the NNLO matching coefficient computed in Ref. [56]. Both are consistent with our ζ_1 and ζ_2 quoted above. As an additional validation of the higher- n matching coefficients, we carried out the calculation in a general R_ξ gauge and verified that the dependence on the gauge parameter cancels in the final expressions.

Furthermore, the logarithmic terms can be checked by the renormalization group (RG) equation

$$\mu^2 \frac{d}{d\mu^2} \zeta_n(t, \mu) = \gamma_n \zeta_n(t, \mu), \quad (3.10)$$

where the

$$\gamma_n = -a_s \sum_{i \geq 0} a_s^i \gamma_{n,i} \quad (3.11)$$

are the anomalous dimensions of the renormalized twist-two operators. The values of the coefficients $\gamma_{n,i}$ are given in Eq. (B.10) and Table 2.

4 Conclusions

We have presented the matching coefficients required to relate the first six non-singlet flowed twist-two operators to the $\overline{\text{MS}}$ scheme through NNLO QCD, providing the perturbative input needed to implement the method proposed in Ref. [33]. The coefficients have already been used to match and determine higher moments of the pion PDF from lattice QCD [49, 50]. Their applicability is not restricted to the pion: they can be used equally for proton PDFs and other hadronic systems. In addition, since moments of off-forward distributions such as generalized parton densities (GPDs) involve non-forward matrix elements of twist-two operators, our results may be relevant for future studies of GPDs based on this approach.

Future work in this direction includes the extension to the singlet sector, whose treatment is technically more involved due to the enlarged operator basis and mixing patterns. We do not expect conceptual obstacles, and the present calculation provides a solid foundation for its determination.

Acknowledgments. A.S. thanks the members of OpenLat for an enjoyable collaboration, in particular Dimitra A. Pefkou, Jangho Kim, and André Walker-Loud for their contributions to the calculation of flowed moments. R.V.H. and J.T.K. acknowledge support by the Deutsche Forschungsgemeinschaft (DFG, German Research Foundation) under grants 460791904 and 396021762 – TRR 257 “Particle Physics Phenomenology after the Higgs Discovery”. A.S. acknowledges funding support from Deutsche Forschungsgemeinschaft (DFG, German Research Foundation) through grant 513989149, and from the National Science Foundation grant PHY-2209185.

A Definition of the gradient flow

Throughout this paper, we work in D -dimensional Euclidean space-time with $D = 4 - 2\epsilon$. The flowed gluon field $B_\mu^a(t)$ is defined by the flow equation [34, 35]

$$\partial_t B_\mu^a = \mathcal{D}_\nu^{ab} G_{\nu\mu}^b + \kappa \mathcal{D}_\mu^{ab} \partial_\nu B_\nu^b, \quad (A.1)$$

and the initial condition

$$B_\mu^a(t=0) = A_\mu^a, \quad (\text{A.2})$$

where A_μ^a is the regular (i.e. unflowed) gluon field,

$$G_{\mu\nu}^a = \partial_\mu B_\nu^a - \partial_\nu B_\mu^a + g_B f^{abc} B_\mu^b B_\nu^c \quad (\text{A.3})$$

is the flowed field-strength tensor,

$$\mathcal{D}_\mu^{ab} = \delta^{ab} \partial_\mu - g_B f^{abc} B_\mu^c \quad (\text{A.4})$$

is the flowed covariant derivative in the adjoint representation, and f^{abc} are the SU(3) structure constants. g_B is the bare strong coupling constant, and κ is a gauge parameter which we set to $\kappa = 1$ throughout our calculation. Our final results for the matching coefficients are independent of this choice though.

The flow equations for the quark fields $\chi(t)$ read [37]

$$\partial_t \chi = \Delta \chi + i\kappa \partial_\mu B_\mu^a \frac{\lambda^a}{2} \chi, \quad \partial_t \bar{\chi} = \bar{\chi} \overleftarrow{\Delta} - i\kappa \bar{\chi} \partial_\mu B_\mu^a \frac{\lambda^a}{2}, \quad (\text{A.5})$$

where the λ^a are the Gell-Mann matrices, and the initial conditions are $\chi(t=0) = \psi$, $\bar{\chi}(t=0) = \bar{\psi}$, where ψ , $\bar{\psi}$ are the regular quark fields. Furthermore,

$$\Delta \chi = \mathcal{D}_\mu \mathcal{D}_\mu \chi, \quad \bar{\chi} \overleftarrow{\Delta} = \bar{\chi} \overleftarrow{\mathcal{D}}_\mu \overleftarrow{\mathcal{D}}_\mu, \quad (\text{A.6})$$

with the flowed covariant derivative in the fundamental representation,

$$\mathcal{D}_\mu = \partial_\mu - ig_B B_\mu^a \frac{\lambda^a}{2}, \quad \overleftarrow{\mathcal{D}}_\mu = \overleftarrow{\partial}_\mu + ig_B B_\mu^a \frac{\lambda^a}{2}. \quad (\text{A.7})$$

The perturbative approach for the solution of these equations has been worked out in Refs. [36, 37]; more details can be found in Ref. [53].

B Renormalization constants

In the GFF, the strong coupling renormalizes in the same way as in regular QCD. We adopt the $\overline{\text{MS}}$ scheme and relate the bare coupling g_B to the renormalized coupling $g(\mu)$ as

$$g_B = \left(\frac{\mu^2 e^{\gamma_E}}{4\pi} \right)^{\epsilon/2} Z_g(a_s(\mu)) g(\mu), \quad a_s(\mu) = \frac{g^2(\mu)}{4\pi^2}, \quad (\text{B.1})$$

with

$$Z_g(a_s) = 1 - a_s \frac{\beta_0}{2\epsilon} + a_s^2 \left(\frac{3\beta_0^2}{8\epsilon^2} - \frac{\beta_1}{4\epsilon} \right) + \mathcal{O}(a_s^3), \quad (\text{B.2})$$

and

$$\beta_0 = \frac{1}{4} \left(\frac{11}{3} C_A - \frac{4}{3} T_R n_f \right), \quad \beta_1 = \frac{1}{16} \left[\frac{34}{3} C_A^2 - \left(4C_F + \frac{20}{3} C_A \right) T_R n_f \right]. \quad (\text{B.3})$$

The parameters C_F , C_A , T_R , and n_f are defined in Section 3.

For the other $\overline{\text{MS}}$ renormalization constants, we use the form

$$Z^{\overline{\text{MS}}}(a_s) = 1 - a_s \frac{\gamma_0}{\epsilon} + a_s^2 \left[\frac{1}{2\epsilon^2} (\gamma_0^2 + \beta_0 \gamma_0) - \frac{\gamma_1}{2\epsilon} \right] + \mathcal{O}(a_s^3), \quad (\text{B.4})$$

with β_0 given in Eq. (B.3), and the coefficients γ_0 , γ_1 to be specified case-by-case.

The renormalization constant of the flowed quark fields in the ringed scheme, defined by Eq. (2.5), is non-minimal and can be written as

$$\overset{\circ}{Z}_\chi = \zeta_\chi(t, \mu) Z_\chi^{\overline{\text{MS}}}, \quad (\text{B.5})$$

where the $\overline{\text{MS}}$ part is given by Eq. (B.4), with γ_0 and γ_1 replaced by [37, 56]

$$\gamma_{\chi,0} = -\frac{3}{4}C_F, \quad \gamma_{\chi,1} = \left(\frac{1}{2} \ln 2 - \frac{223}{96} \right) C_A C_F + \left(\frac{3}{32} + \frac{1}{2} \ln 2 \right) C_F^2 + \frac{11}{24} C_F T_R n_f. \quad (\text{B.6})$$

The finite part reads

$$\begin{aligned} \zeta_\chi(t, \mu) = & 1 - a_s \left(\gamma_{\chi,0} L_{\mu t} + \frac{3}{4} C_F \ln 3 + C_F \ln 2 \right) \\ & + a_s^2 \left\{ \frac{\gamma_{\chi,0}}{2} (\gamma_{\chi,0} - \beta_0) L_{\mu t}^2 + \left[\gamma_{\chi,0} (\beta_0 - \gamma_{\chi,0}) \ln 3 \right. \right. \\ & \left. \left. + \frac{4}{3} \gamma_{\chi,0} (\beta_0 - \gamma_{\chi,0}) \ln 2 - \gamma_{\chi,1} \right] L_{\mu t} + \frac{c_\chi^{(2)}}{16} \right\} + \mathcal{O}(a_s^3), \end{aligned} \quad (\text{B.7})$$

with $L_{\mu t}$ defined in Eq. (3.3), and [53]

$$c_\chi^{(2)} = C_A C_F c_{\chi,A} + C_F^2 c_{\chi,F} + C_F T_R n_f c_{\chi,R}, \quad (\text{B.8})$$

where

$$\begin{aligned} c_{\chi,A} &= -23.7947, & c_{\chi,F} &= 30.3914, \\ c_{\chi,R} &= -\frac{131}{18} + \frac{46}{3} \zeta_2 + \frac{944}{9} \ln 2 + \frac{160}{3} \ln^2 2 - \frac{172}{3} \ln 3 + \frac{104}{3} \ln 2 \ln 3 \\ & - \frac{178}{3} \ln^2 3 + \frac{8}{3} \text{Li}_2(1/9) - \frac{400}{3} \text{Li}_2(1/3) + \frac{112}{3} \text{Li}_2(3/4) = -3.92255 \dots \end{aligned} \quad (\text{B.9})$$

The $\overline{\text{MS}}$ renormalization constants Z_n of the twist-two operators are determined by Eq. (B.4), with γ_i replaced by the Mellin moments $\gamma_{n,i}$ of the splitting functions which are known through three loops for arbitrary values of n [5, 6]. For the operators relevant to this paper, we only require the non-singlet two-loop expressions up to $n = 6$ [74–76], which we write as

$$\gamma_{n,0} = C_F a_n, \quad \gamma_{n,1} = b_n C_F^2 + c_n C_F C_A + d_n C_F n_f T_R, \quad (\text{B.10})$$

where the relevant values of the coefficients a_n, \dots, d_n are given in Table 2. The case $n = 1$ is not included in Table 2, because $\gamma_1 = 0$ to all orders due to vector current conservation.

Table 2: Analytical values for the coefficients of $\gamma_{n,0}$ and $\gamma_{n,1}$ for the values of n relevant to our renormalization assuming the parametrization Eq. (B.10).

n	a_n	b_n	c_n	d_n
2	$\frac{2}{3}$	$-\frac{7}{27}$	$\frac{47}{54}$	$-\frac{8}{27}$
3	$\frac{25}{24}$	$-\frac{2035}{6912}$	$\frac{535}{432}$	$-\frac{415}{864}$
4	$\frac{157}{120}$	$-\frac{287303}{864000}$	$\frac{16157}{10800}$	$-\frac{13271}{21600}$
5	$\frac{91}{60}$	$-\frac{2891}{8000}$	$\frac{73223}{43200}$	$-\frac{7783}{10800}$
6	$\frac{709}{420}$	$-\frac{3173311}{8232000}$	$\frac{157415}{84672}$	$-\frac{428119}{529200}$

C Ancillary file

We provide the main results of this paper in computer readable form as ancillary files `Zeta.m` in *Mathematica* and `Zeta.py` in *Python* format. A list of the provided quantities is given in Table 3. The matching coefficients ζ are provided both in the $\overline{\text{MS}}$ scheme and the ringed scheme for the flowed quark fields. Switching between the two is possible by setting the variable `Xzetachi` to 0 or 1 to get the $\overline{\text{MS}}$ or the ringed scheme, respectively. All variables and functions which are used in the ancillary files are collected in Table 4. The coefficients $c_\chi^{(2)}$ appearing in the ringed scheme, see Eq. (B.8), are represented by the symbol `C2` and the function `chi2(nf)` in `Zeta.m` and `Zeta.py` file, respectively. In the former, its value is contained in the replacement rule `ReplaceC2`, see Eqs. (B.8) and (B.9). We also provide the anomalous dimensions γ_n for general n in the notation of Eqs. (B.10) and (3.11) [76]. For $n = 2, \dots, 6$, explicit results are given in Table 2.

Table 3: The expressions of the ancillary files `Zeta.m` and `Zeta.py` that encode the main results of this paper. The notation of the variables should be self-explanatory; more details are given in the header of these files.

<code>Zeta.m</code>	<code>Zeta.py</code>	meaning	reference
<code>zeta1</code>	<code>zeta_1(alpha_s,nf,mu,t,0a=2)</code>	$\zeta_1(t, \mu)$	Eq. (3.4)
\vdots	\vdots	\vdots	\vdots
<code>zeta6</code>	<code>zeta_6(alpha_s,nf,mu,t,0a=2)</code>	$\zeta_6(t, \mu)$	Eq. (3.4)
<code>gamma[n_]</code>	<code>gamma(n,alpha_s,nf,0a=2)</code>	γ_n	Eqs. (B.10) and (3.11)

Table 4: Notation for the variables in the ancillary files.

Zeta.m	Zeta.py	meaning	reference
cf	CF	C_F	Eq. (3.1)
ca	CA	C_A	Eq. (3.1)
tr	TR	T_R	Eq. (3.1)
Lmut	Lmut	$L_{\mu t}$	Eq. (3.3)
as	a_s	a_s	Eq. (3.2)
alpha_s	alpha_s	α_s	πa_s
nf	nf	n_f	Section 2.2

References

- [1] J. C. Collins, D. E. Soper, and G. F. Sterman, “Factorization of Hard Processes in QCD,” *Adv. Ser. Direct. High Energy Phys.* **5** (1989) 1–91, [arXiv:hep-ph/0409313](#).
- [2] V. N. Gribov and L. N. Lipatov, “Deep inelastic ep scattering in perturbation theory,” *Sov. J. Nucl. Phys.* **15** (1972) 438–450.
- [3] G. Altarelli and G. Parisi, “Asymptotic Freedom in Parton Language,” *Nucl. Phys. B* **126** (1977) 298–318.
- [4] Y. L. Dokshitzer, “Calculation of the structure functions for deep inelastic scattering and e^+e^- annihilation by perturbation theory in quantum chromodynamics,” *Sov. Phys. JETP* **46** (1977) 641–653.
- [5] S. Moch, J. A. M. Vermaseren, and A. Vogt, “The three-loop splitting functions in QCD: The nonsinglet case,” *Nucl. Phys. B* **688** (2004) 101–134, [arXiv:hep-ph/0403192](#).
- [6] A. Vogt, S. Moch, and J. A. M. Vermaseren, “The three-loop splitting functions in QCD: The singlet case,” *Nucl. Phys. B* **691** (2004) 129–181, [arXiv:hep-ph/0404111](#).
- [7] T. Gehrmann, A. von Manteuffel, V. Sotnikov, and T.-Z. Yang, “Complete N_f^2 contributions to four-loop pure-singlet splitting functions,” *JHEP* **01** (2024) 029, [arXiv:2308.07958 \[hep-ph\]](#).
- [8] G. Falcioni, F. Herzog, S. Moch, J. Vermaseren, and A. Vogt, “The double fermionic contribution to the four-loop quark-to-gluon splitting function,” *Phys. Lett. B* **848** (2024) 138351, [arXiv:2310.01245 \[hep-ph\]](#).
- [9] T. Gehrmann, A. von Manteuffel, V. Sotnikov, and T.-Z. Yang, “The $N_f C_F^3$ contribution to the non-singlet splitting function at four-loop order,” *Phys. Lett. B* **849** (2024) 138427, [arXiv:2310.12240 \[hep-ph\]](#).

- [10] G. Falcioni, F. Herzog, S. Moch, A. Pelloni, and A. Vogt, “Four-loop splitting functions in QCD – the gluon-gluon case –,” *Phys. Lett. B* **860** (2025) 139194, [arXiv:2410.08089 \[hep-ph\]](#).
- [11] G. Falcioni, F. Herzog, S. Moch, A. Pelloni, and A. Vogt, “Four-loop splitting functions in QCD – The quark-to-gluon case,” *Phys. Lett. B* **856** (2024) 138906, [arXiv:2404.09701 \[hep-ph\]](#).
- [12] B. A. Kniehl and V. N. Velizhanin, “Four-Loop Anomalous Dimension of Flavor Nonsinglet Twist-Two Operator of General Lorentz Spin in QCD: $\zeta(3)$ Term,” *Phys. Rev. Lett.* **134** no. 13, (2025) 131901, [arXiv:2503.20422 \[hep-ph\]](#).
- [13] B. A. Kniehl, S. Moch, V. N. Velizhanin, and A. Vogt, “Flavor nonsinglet splitting functions at four loops in QCD: Fermionic contributions,” *Phys. Rev. Lett.* **135** no. 7, (2025) 071902, [arXiv:2505.09381 \[hep-ph\]](#).
- [14] S. Amoroso *et al.*, “Higgs boson cross-section measurements and constraints on parton distribution functions with the ATLAS detector at the LHC,” *JHEP* **07** (2022) 032, [arXiv:2207.10607 \[hep-ex\]](#).
- [15] R. Abir *et al.*, “The case for an EIC Theory Alliance: Theoretical challenges of the EIC,” [arXiv:2305.14572 \[hep-ph\]](#).
- [16] **LHeC, FCC-he Study Group** Collaboration, P. Agostini *et al.*, “The Large Hadron–Electron Collider at the HL-LHC,” *J. Phys. G* **48** no. 11, (2021) 110501, [arXiv:2007.14491 \[hep-ex\]](#).
- [17] K.-F. Liu and S.-J. Dong, “Origin of difference between anti-d and anti-u partons in the nucleon,” *Phys. Rev. Lett.* **72** (1994) 1790–1793, [arXiv:hep-ph/9306299](#).
- [18] U. Aglietti, M. Ciuchini, G. Corbo, E. Franco, G. Martinelli, and L. Silvestrini, “Model independent determination of the shape function for inclusive B decays and of the structure functions in DIS,” *Phys. Lett. B* **432** (1998) 411–420, [arXiv:hep-ph/9804416](#).
- [19] W. Detmold and C. J. D. Lin, “Deep-inelastic scattering and the operator product expansion in lattice QCD,” *Phys. Rev. D* **73** (2006) 014501, [arXiv:hep-lat/0507007](#).
- [20] X. Ji, “Parton physics on a Euclidean lattice,” *Phys. Rev. Lett.* **110** no. 26, (2013) 262002, [arXiv:1305.1539 \[hep-ph\]](#).
- [21] A. V. Radyushkin, “Quasi-parton distribution functions, momentum distributions, and pseudo-parton distribution functions,” *Phys. Rev. D* **96** no. 3, (2017) 034025, [arXiv:1705.01488 \[hep-ph\]](#).
- [22] K. Orginos, A. Radyushkin, J. Karpie, and S. Zafeiropoulos, “Lattice QCD exploration of parton pseudo-distribution functions,” *Phys. Rev. D* **96** no. 9, (2017) 094503, [arXiv:1706.05373 \[hep-ph\]](#).

- [23] Y.-Q. Ma and J.-W. Qiu, “Extracting parton distribution functions from lattice QCD calculations,” *Phys. Rev. D* **98** no. 7, (2018) 074021, [arXiv:1404.6860](#) [hep-ph].
- [24] V. Braun and D. Müller, “Exclusive processes in position space and the pion distribution amplitude,” *Eur. Phys. J. C* **55** (2008) 349–361, [arXiv:0709.1348](#) [hep-ph].
- [25] A. J. Chambers, R. Horsley, Y. Nakamura, H. Perlt, P. E. L. Rakow, G. Schierholz, A. Schiller, K. Somfleth, R. D. Young, and J. M. Zanotti, “Nucleon structure functions from operator product expansion on the lattice,” *Phys. Rev. Lett.* **118** no. 24, (2017) 242001, [arXiv:1703.01153](#) [hep-lat].
- [26] X. Gao, W.-Y. Liu, and Y. Zhao, “Parton distributions from boosted fields in the Coulomb gauge,” *Phys. Rev. D* **109** no. 9, (2024) 094506, [arXiv:2306.14960](#) [hep-ph].
- [27] A. S. Kronfeld and D. M. Photiadis, “Phenomenology on the lattice: Composite operators in lattice gauge theory,” *Phys. Rev. D* **31** (1985) 2939.
- [28] G. Martinelli and C. T. Sachrajda, “Pion structure functions from lattice QCD,” *Phys. Lett. B* **196** (1987) 184–190.
- [29] G. Martinelli and C. T. Sachrajda, “A lattice calculation of the pion’s form-factor and structure function,” *Nucl. Phys. B* **306** (1988) 865–889.
- [30] M. Göckeler, R. Horsley, E.-M. Ilgenfritz, H. Perlt, P. E. L. Rakow, G. Schierholz, and A. Schiller, “Lattice operators for moments of the structure functions and their transformation under the hypercubic group,” *Phys. Rev. D* **54** (1996) 5705–5714, [arXiv:hep-lat/9602029](#).
- [31] **ETM** Collaboration, C. Alexandrou, S. Bacchio, I. Cloet, M. Constantinou, K. Hadjiyiannakou, G. Koutsou, and C. Lauer, “Mellin moments $\langle x \rangle$ and $\langle x^2 \rangle$ for the pion and kaon from lattice QCD,” *Phys. Rev. D* **103** no. 1, (2021) 014508, [arXiv:2010.03495](#) [hep-lat].
- [32] **ETM** Collaboration, C. Alexandrou, S. Bacchio, I. Cloët, M. Constantinou, K. Hadjiyiannakou, G. Koutsou, and C. Lauer, “Pion and kaon $\langle x^3 \rangle$ from lattice QCD and PDF reconstruction from Mellin moments,” *Phys. Rev. D* **104** no. 5, (2021) 054504, [arXiv:2104.02247](#) [hep-lat].
- [33] A. Shindler, “Moments of parton distribution functions of any order from lattice QCD,” *Phys. Rev. D* **110** no. 5, (2024) L051503, [arXiv:2311.18704](#) [hep-lat].
- [34] R. Narayanan and H. Neuberger, “Infinite N phase transitions in continuum Wilson loop operators,” *JHEP* **03** (2006) 064, [arXiv:hep-th/0601210](#).
- [35] M. Lüscher, “Properties and uses of the Wilson flow in lattice QCD,” *JHEP* **08** (2010) 071, [arXiv:1006.4518](#) [hep-lat]. [Erratum: *JHEP* 03, 092 (2014)].

- [36] M. Lüscher and P. Weisz, “Perturbative analysis of the gradient flow in non-abelian gauge theories,” *JHEP* **02** (2011) 051, [arXiv:1101.0963 \[hep-th\]](#).
- [37] M. Lüscher, “Chiral symmetry and the Yang–Mills gradient flow,” *JHEP* **04** (2013) 123, [arXiv:1302.5246 \[hep-lat\]](#).
- [38] H. Suzuki, “Energy–momentum tensor from the Yang–Mills gradient flow,” *PTEP* **2013** (2013) 083B03, [arXiv:1304.0533 \[hep-lat\]](#). [Erratum: *PTEP* 2015, 079201 (2015)].
- [39] M. Lüscher, “Future applications of the Yang–Mills gradient flow in lattice QCD,” *PoS LATTICE2013* (2014) 016, [arXiv:1308.5598 \[hep-lat\]](#).
- [40] A. Shindler, “Unlocking higher-order moments of parton distribution functions from lattice QCD,” *PoS DIS2024* (2025) 237, [arXiv:2410.00198 \[hep-lat\]](#).
- [41] T. Iritani, M. Kitazawa, H. Suzuki, and H. Takaura, “Thermodynamics in quenched QCD: energy–momentum tensor with two-loop order coefficients in the gradient-flow formalism,” *PTEP* **2019** no. 2, (2019) 023B02, [arXiv:1812.06444 \[hep-lat\]](#).
- [42] R. Harlander, M. D. Rizik, J. Borgulat, and A. Shindler, “Two-loop matching of the chromo-magnetic dipole operator with the gradient flow,” *PoS LATTICE2022* (2023) 313, [arXiv:2212.09824 \[hep-lat\]](#).
- [43] M. Black, R. Harlander, F. Lange, A. Rago, A. Shindler, and O. Witzel, “Gradient flow renormalisation for meson mixing and lifetimes,” *PoS LATTICE2024* (2025) 243, [arXiv:2409.18891 \[hep-lat\]](#).
- [44] F. Cuteri, A. Francis, P. Fritzsche, G. Pederiva, A. Rago, A. Shindler, A. Walker-Loud, and S. Zafeiropoulos, “Benchmark continuum limit results for spectroscopy with stabilized Wilson fermions,” *PoS LATTICE2022* (2023) 074, [arXiv:2212.11048 \[hep-lat\]](#).
- [45] F. Cuteri, A. S. Francis, P. Fritzsche, G. Pederiva, A. Rago, A. Shindler, A. Walker-Loud, and S. Zafeiropoulos, “Gauge generation and dissemination in OpenLat,” *PoS LATTICE2022* (2023) 426, [arXiv:2212.07314 \[hep-lat\]](#).
- [46] A. S. Francis, F. Cuteri, P. Fritzsche, G. Pederiva, A. Rago, A. Shindler, A. Walker-Loud, and S. Zafeiropoulos, “Properties, ensembles and hadron spectra with Stabilised Wilson Fermions,” *PoS LATTICE2021* (2022) 118, [arXiv:2201.03874 \[hep-lat\]](#).
- [47] A. Francis, F. Cuteri, P. Fritzsche, G. Pederiva, A. Rago, A. Shindler, A. Walker-Loud, and S. Zafeiropoulos, “Progress in generating gauge ensembles with Stabilized Wilson Fermions,” *PoS LATTICE2023* (2024) 048, [arXiv:2312.11298 \[hep-lat\]](#).
- [48] A. Francis, P. Fritzsche, R. Karur, J. Kim, G. Pederiva, D. A. Pefkou, A. Rago, A. Shindler, A. Walker-Loud, and S. Zafeiropoulos, “Probing higher moments of pion parton distribution functions,” *PoS LATTICE2024* (2025) 336, [arXiv:2412.01750 \[hep-lat\]](#).

- [49] A. Francis, P. Fritzscht, R. Karur, J. Kim, G. Pederiva, D. A. Pefkou, A. Rago, A. Shindler, A. Walker-Loud, and S. Zafeiropoulos, “Moments of parton distributions functions of the pion from lattice QCD using gradient flow,” [arXiv:2510.26738](#) [hep-lat].
- [50] A. Francis *et al.*, “Gradient flow for parton distribution functions: first application to the pion,” [arXiv:2509.02472](#) [hep-lat].
- [51] K. Hieda, H. Makino, and H. Suzuki, “Proof of the renormalizability of the gradient flow,” *Nucl. Phys. B* **918** (2017) 23–51, [arXiv:1604.06200](#) [hep-lat].
- [52] H. Makino and H. Suzuki, “Lattice energy–momentum tensor from the Yang–Mills gradient flow—inclusion of fermion fields,” *PTEP* **2014** (2014) 063B02, [arXiv:1403.4772](#) [hep-lat]. [Erratum: PTEP 2015, 079202 (2015)].
- [53] J. Artz, R. V. Harlander, F. Lange, T. Neumann, and M. Prausa, “Results and techniques for higher order calculations within the gradient-flow formalism,” *JHEP* **06** (2019) 121, [arXiv:1905.00882](#) [hep-lat]. [Erratum: JHEP 10, 032 (2019)].
- [54] S. G. Gorishnii, S. A. Larin, and F. V. Tkachov, “The algorithm for OPE coefficient functions in the MS scheme,” *Phys. Lett. B* **124** (1983) 217–220.
- [55] S. G. Gorishnii and S. A. Larin, “Coefficient Functions of Asymptotic Operator Expansions in Minimal Subtraction Scheme,” *Nucl. Phys. B* **283** (1987) 452.
- [56] R. V. Harlander, Y. Kluth, and F. Lange, “The two-loop energy–momentum tensor within the gradient-flow formalism,” *Eur. Phys. J. C* **78** no. 11, (2018) 944, [arXiv:1808.09837](#) [hep-lat]. [Erratum: Eur.Phys.J.C 79, 858 (2019)].
- [57] G. ’t Hooft and M. J. G. Veltman, “Regularization and renormalization of gauge fields,” *Nucl. Phys. B* **44** (1972) 189–213.
- [58] P. Nogueira, “Automatic Feynman graph generation,” *J. Comput. Phys.* **105** (1993) 279–289.
- [59] P. Nogueira, “Abusing QGRAF,” *Nucl. Instrum. Meth. A* **559** (2006) 220–223.
- [60] R. Harlander, T. Seidensticker, and M. Steinhauser, “Corrections of $O(\alpha\alpha_s)$ to the decay of the Z boson into bottom quarks,” *Phys. Lett. B* **426** (1998) 125–132, [arXiv:hep-ph/9712228](#).
- [61] T. Seidensticker, “Automatic application of successive asymptotic expansions of Feynman diagrams,” in *6th International Workshop on New Computing Techniques in Physics Research: Software Engineering, Artificial Intelligence Neural Nets, Genetic Algorithms, Symbolic Algebra, Automatic Calculation*. 5, 1999. [arXiv:hep-ph/9905298](#).
- [62] M. Gerlach, F. Herren, and M. Lang, “tapir: A tool for topologies, amplitudes, partial fraction decomposition and input for reductions,” *Comput. Phys. Commun.* **282** (2023) 108544, [arXiv:2201.05618](#) [hep-ph].

- [63] M. Gerlach, “Three-loop topology analysis of neutral B -meson mixing with tapir,” *J. Phys. Conf. Ser.* **2438** no. 1, (2023) 012156, [arXiv:2205.07483 \[hep-ph\]](#).
- [64] J. A. M. Vermaseren, “New features of FORM,” [arXiv:math-ph/0010025](#).
- [65] B. Ruijl, T. Ueda, and J. Vermaseren, “FORM version 4.2,” [arXiv:1707.06453 \[hep-ph\]](#).
- [66] K. G. Chetyrkin and F. V. Tkachov, “Integration by parts: The algorithm to calculate β -functions in 4 loops,” *Nucl. Phys. B* **192** (1981) 159–204.
- [67] P. Maierhöfer, J. Usovitsch, and P. Uwer, “Kira—A Feynman integral reduction program,” *Comput. Phys. Commun.* **230** (2018) 99–112, [arXiv:1705.05610 \[hep-ph\]](#).
- [68] J. Klappert, F. Lange, P. Maierhöfer, and J. Usovitsch, “Integral reduction with Kira 2.0 and finite field methods,” *Comput. Phys. Commun.* **266** (2021) 108024, [arXiv:2008.06494 \[hep-ph\]](#).
- [69] J. Klappert and F. Lange, “Reconstructing rational functions with FireFly,” *Comput. Phys. Commun.* **247** (2020) 106951, [arXiv:1904.00009 \[cs.SC\]](#).
- [70] J. Klappert, S. Y. Klein, and F. Lange, “Interpolation of dense and sparse rational functions and other improvements in FireFly,” *Comput. Phys. Commun.* **264** (2021) 107968, [arXiv:2004.01463 \[cs.MS\]](#).
- [71] R. V. Harlander, S. Y. Klein, and M. Lipp, “FeynGame,” *Comput. Phys. Commun.* **256** (2020) 107465, [arXiv:2003.00896 \[physics.ed-ph\]](#).
- [72] L. Bündgen, R. V. Harlander, S. Y. Klein, and M. C. Schaaf, “FeynGame 3.0,” *Comput. Phys. Commun.* **314** (2025) 109662, [arXiv:2501.04651 \[hep-ph\]](#).
- [73] J. Borgulat, R. V. Harlander, J. T. Kohnen, and F. Lange, “Short-flow-time expansion of quark bilinears through next-to-next-to-leading order QCD,” *JHEP* **05** (2024) 179, [arXiv:2311.16799 \[hep-lat\]](#).
- [74] D. J. Gross and F. Wilczek, “Asymptotically free gauge theories. II,” *Phys. Rev. D* **9** (1974) 980–993.
- [75] E. G. Floratos, D. A. Ross, and C. T. Sachrajda, “Higher order effects in asymptotically free gauge theories: The anomalous dimensions of Wilson operators,” *Nucl. Phys. B* **129** (1977) 66–88. [Erratum: *Nucl.Phys.B* 139, 545–546 (1978)].
- [76] A. Gonzalez-Arroyo, C. Lopez, and F. J. Yndurain, “Second order contributions to the structure functions in deep inelastic scattering. 1. Theoretical calculations,” *Nucl. Phys. B* **153** (1979) 161–186.